# Biaxial order and a rotation of the minor director in the nematic phase of an organo-siloxane tetrapode by the electric field

K. Merkel, M. Nagaraj, A. Kocot, A. Kohlmeier, G. H. Mehl, and J. K. Vij

Citation: The Journal of Chemical Physics **136**, 094513 (2012); doi: 10.1063/1.3690108
View online: http://dx.doi.org/10.1063/1.3690108
View Table of Contents: http://scitation.aip.org/content/aip/journal/jcp/136/9?ver=pdfcov
Published by the AIP Publishing

# Biaxial order and a rotation of the minor director in the nematic phase of an organo-siloxane tetrapode by the electric field

K. Merkel,[1,2] M. Nagaraj,[2] A. Kocot,[2,3] A. Kohlmeier,[4] G. H. Mehl,[4] and J. K. Vij[2,a)]
[1]*Central Mining Institute, Plac Gwarkow 1, Katowice, Poland*
[2]*Laboratory of Advanced Materials, Department of Electronic and Electrical Engineering, Trinity College, University of Dublin, Dublin 2, Ireland*
[3]*Institute of Physics, University of Silesia, Katowice, Poland*
[4]*Department of Chemistry, University of Hull, Cottingham Road, Hull HU6 7RX, United Kingdom*

(Received 7 January 2012; accepted 10 February 2012; published online 7 March 2012)

Biaxiality in the nematic phase for a liquid crystalline tetrapode made up of organo-siloxanes mesogens is investigated using polarized infrared spectroscopy. An ordering of the minor director for the homeotropically aligned sample is found to depend on the amplitude of the in-plane electric field. On increasing the in-plane electric field, the minor director, lying initially along the rubbing direction, rotates to the direction of the applied field. The scalar order parameters of the second rank tensor are found to depend significantly on the strength of the electric field. A most significant increase is found in the nematic order parameter and in the parameter that characterizes the phase biaxiality.
 [http://dx.doi.org/10.1063/1.3690108]

## I. INTRODUCTION

Liquid crystalline tetrapodes are composed of four mesogenic arms linked to the siloxane core through flexible spacers forming a quasiflat platelet. Each of the mesogens of the tetrapode on its own is also liquid crystalline. In order to achieve an optimized packing, the mesogens are tilted in the plane of the platelet. The nematic phase of tetrapode system consists of an interdigitation of the laterally attached mesogenic units which may belong to the neighboring tetrapodes. This interdigitation hinders the rotational freedom of the mesogenic units and may lead to a biaxial nematic phase. The biaxiality is determined by the anisotropy of its geometerical frame, the angle between the mesogenic groups and the axes in that frame. Biaxiality in the nematic phase of such systems with asymmetric and symmetric mesogenic units was first discovered by Merkel *et al.*[1] using polarized infrared (IR) spectroscopy. The NMR spectroscopy of one of the two tetrapode systems showed two distinct nematic regions, one with a vanishing asymmetry parameter corresponding to the uniaxial nematic phase and second with a significant temperature dependent asymmetry parameter corresponding to the biaxial nematic phase.[2,3] Biaxiality in its nematic phase was also confirmed by dynamic light scattering[4] where the central Si atom of the tetrapode molecule was replaced by Ge; however the chains remained siloxanes as before. Recently, molecular theory for the relative stability of the uniaxial and biaxial nematic phases in tetrapode-like systems was given by Gorkunov *et al.*[5]

Most of the applications of liquid crystals are based on using their anisotropic properties and their large dependencies on pressure, temperature, and external fields. Basically, the macroscopic anisotropic properties of liquid crystals are governed by their molecular behavior, alignment, and the orientational order of the constituent molecules.[6–10] In this paper, we use polarized IR spectroscopy to quantitatively determine the scalar order parameters and describe how these order parameters are influenced by the electric field. We examine the relevant theory, and then focus on to the experimental results in the context of theoretical predictions. The chemical structure, the phase sequence and the transition temperatures of the tetrameric siloxane dendritic liquid crystal are given in Fig. 1(a).

## II. POLARIZED INFRARED SPECTROSCOPY

The orientation of a rigid biaxial molecule can be specified by unit vectors $\boldsymbol{a}$ and $\boldsymbol{b}$ in the direction of the primary ("long") and secondary ("short") molecular axes, respectively. The third molecular axis is then specified by the unit vector $\boldsymbol{c}$; this is orthogonal to both vectors $\boldsymbol{a}$ and $\boldsymbol{b}$. In the biaxial nematic phase, there exist three mutually orthogonal macroscopic directions specified by the primary direction $n$ and two secondary orthogonal directions, $m$ and $h$. The unit vectors $\boldsymbol{a}$, $\boldsymbol{b}$, and $\boldsymbol{c}$, which form the molecular frame, can be expressed in the macroscopic $\{n, m, h\}$ frame of coordinates. Since the pioneering work of Straley,[11] the following two tensor order parameters: $Q_{ij} = \langle a_i a_j - 1/3\delta_{ij}\rangle$ and $B_{ij} = \langle b_i b_j - c_i c_j\rangle$ are used to describe the thermodynamic properties of biaxial nematics. These two tensor order parameters **Q** and **B**, however, are generally insufficient for the description of a biaxial phase with the orthorhombic symmetry ($D_{2h}$) as shown by Gorkunov *et al.*[5] In principle a low symmetry biaxial nematic phase with $C_{2h}$ symmetry may also exist.[12]

The absorbance profile vs. the angle of polarization of the IR beam can in principle give a direct evidence of departure from the orthorhombic symmetry. Lower symmetry shall break the overall symmetry of the absorbance profile as shown.[13] The absorbance profiles of the bands 762 $cm^{-1}$

a)Author to whom correspondence should be addressed. Electronic mail: jvij@tcd.ie.

 

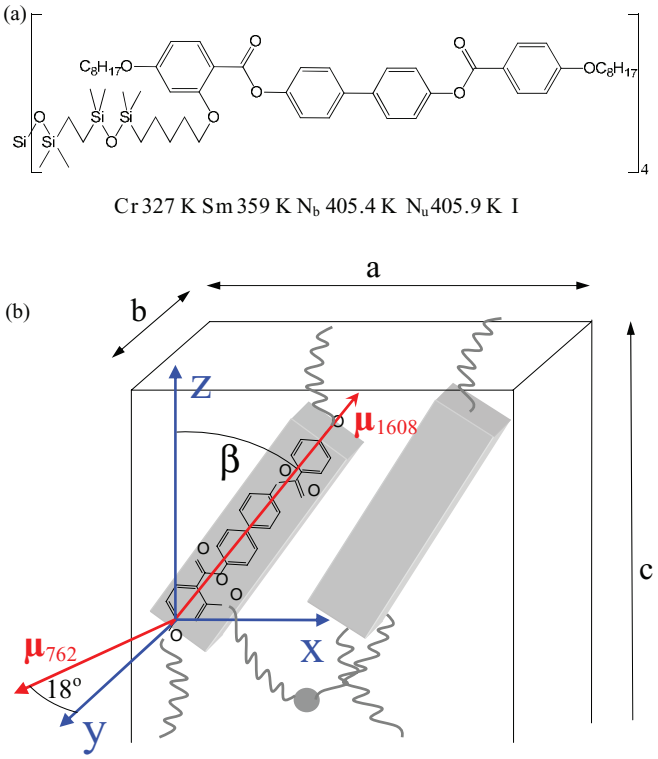


FIG. 1. (a) Molecular structure of the tetrapode with a symmetrical mesogen. Transition temperatures are taken from Ref. 1. (b) Molecular frame of reference of the tetrapode. Orientation of the transition dipoles corresponding to the bands:phenyl stretching vibration 1608 $cm^{-1}$ and deformation of the phenyl ring 762 $cm^{-1}$ are shown.

and 1737 $cm^{-1}$ for the studied tetrapode system are exactly orthogonal to that of 1608 $cm^{-1}$ band within the experimental error despite the fact that their corresponding transition dipoles are not perpendicular to the longitudinal dipole moment. This shows that macroscopically the symmetry is not lower than $D_{2h}$. It implies that the local order such as "SmC like order"[6] does not necessarily break the phase symmetry. Hence, the orientational molecular order parameters discussed in this paper are defined by the three diagonal Saupe ordering matrices $S^i_{\alpha\beta} = \langle \frac{1}{2}(3l_{i,\alpha}l_{i,\beta} - \delta_{\alpha\beta})\rangle$, one for each of the three laboratory axes, $i = X, Y, Z$. $\alpha, \beta = x, y, z$; $l_{i,\alpha}$ is the cosine of the angle between the molecular $\alpha$ and the laboratory or the phase axes $i$. Similarly, $l_{i,\beta}$ is the cosine of the angle between the molecular $\beta$ and the phase axes, $i$.

The tensor order parameter $S^i_{\alpha\beta}$ leads to four scalar order parameters defined as follows:

$$S = S^Z_{zz}, \quad D = S^Z_{xx} - S^Z_{yy}, \quad P = S^X_{zz} - S^Y_{zz}$$
$$C = D' - D'' = \left(S^X_{xx} - S^X_{yy}\right) - \left(S^Y_{xx} - S^Y_{yy}\right). \tag{1}$$

The analysis for determining a complete set of four scalar order parameters presented here is valid for the orthorhombic or the $D_{2h}$ symmetry of the system. The experimental determination of biaxiality is therefore based on this symmetry. In an orientationally ordered sample, the absorbance components are dependent on the angle between the alignment axis and polarization direction of the incident beam of IR. At a microscopic level, the infrared absorption depends on the projections of a molecular transition dipole moment, $\mu_i$, of a particular absorption band on the principal axes. If the effects of the molecular interactions and the local field are neglected, then the absorbance components along the principal laboratory axes can be written down in terms of the components of the dipole moment along the molecular axes and the four scalar order parameters defined by the Saupe ordering matrices.[7] The orientational ordering for the tetrapodes has already been investigated in a planar cell;[14] nevertheless, such a geometry is not suitable for detecting the biaxiality in its nematic phase. It is convenient, however to measure the absorbance components of a homeotropically aligned cell and to relate the anisotropy in the $A_X$ and $A_Y$ components to the phase biaxiality parameters, $P$ and $C$. The sum of these components normalized by the absorbance in the isotropic phase is related to the uniaxial order parameters, $S$ and $D$, and the difference leads to $P$ and $C$ as given below:

$$(A_X + A_Y)/2A_0 = 1 - S\left[(l_i)^2_z - \frac{1}{2}\left((l_i)^2_x + (l_i)^2_y\right)\right] - \frac{1}{2}D\left((l_i)^2_x - (l_i)^2_y\right)$$
$$(A_X - A_Y)/2A_0 = P\left[(l_i)^2_z - \frac{1}{2}\left((l_i)^2_x + (l_i)^2_y\right)\right] - \frac{1}{2}C\left((l_i)^2_x - (l_i)^2_y\right), \tag{2}$$

where

$$A_0 = \frac{1}{3}(A_X + A_Y + A_Z). \tag{3}$$

$A_0$ is the mean absorbance; $(l_i)_\alpha$ ($\alpha = x, y, z$ of the molecular frame) are the average direction cosines of the transition dipole moment, $\mu_i$, of the $i$th absorption band, averaged over all conformers. A complete procedure for determining $S$, $P$, $D$, and $C$ from the experimental measurements of the absorbance components (also see Sec. III) at different temperatures is given in Ref. 15. $A_X$ and $A_Y$ can be measured using a homeotropic cell and $A_Z$ is taken from the measurements of the planar cell. $A_0$ is the absorbance in the isotropic phase.

## III. EXPERIMENT

In order to obtain the homeotropic orientation of the molecules, the windows (KBr) of the cell are spin coated with an alignment solution AL60702 (JSR Korea) and both are rubbed in one direction. The cells for the switching experiment are prepared by introducing a pair of aluminium stripe electrodes (2 mm wide), with a gap of 225 $\mu$m, placed on the plane of the bottom substrate. The edges of the stripe electrodes make an angle 45° to the rubbing direction. The foil acts as spacer as well as the in-plane electrodes for the cell. The thickness of the cell so fabricated was determined to be 5.2 $\mu$m from measurements on the interference fringes formed by successive reflections from the two faces of the cell of IR beam. The infrared spectra are recorded using a Bio-Rad FTS 6000 spectrometer equipped with UMA500 IR microscope with a resolution of 2 $cm^{-1}$ and these spectra are averaged over 64 scans. An IR-KRS5 grid polariser is used to polarize the IR beam. The polarized IR spectra are measured

as a function of the polariser rotation angle. In addition, a planar cell of thickness 1.7 $\mu$m is also prepared, electrodes of which are coated with a planar alignment solution (RN-1775, Nissan Chemicals, Japan) and rubbed in one direction only.

## IV. THE DIELECTRIC ANISOTROPY OF THE TETRAPODE SYSTEM

The dielectric anisotropy defined as $\Delta\varepsilon' = \varepsilon'_Z - \frac{1}{2}(\varepsilon'_X + \varepsilon'_Y)$ and the dielectric biaxiality defined as $\Delta\varepsilon'_\perp = \varepsilon'_Y - \varepsilon'_X$, are calculated from the dielectric measurements of the tetrapode system. $\varepsilon'_X$, $\varepsilon'_Y$, and $\varepsilon'_Z$ are the three components in the laboratory frame as the real parts of the complex relative permittivity at the frequency of the measuring field. Measurements were made for weak probe fields at a frequency of 1 kHz. $\varepsilon'_Z$ is measured using a homeotropic cell and $\varepsilon'_X$ and $\varepsilon'_Y$ are measured using a planar cell (cell thickness = 1.7 $\mu$m). The alignment of the major director in a planar cell is obtained by applying a magnetic field of 1.8 T and an electric field of up to 6 V/$\mu$m is applied perpendicular to the long axis to orient the secondary director along which lies the transverse dipole moment. Permittivity so measured is $\varepsilon'_Y$. For weak fields in the range 0.1 − 0.6 V/$\mu$m, the permittivity measured is $\frac{1}{2}(\varepsilon'_X + \varepsilon'_Y)$. The three components of permittivity can thus be determined. From these measurements, the calculated value of the dielectric anisotropy $\Delta\varepsilon'$ at a frequency of 1 kHz and temperature of 373 K for the tetrapode system is found to be –0.22 ± 0.02, and the dielectric biaxiality $\Delta\varepsilon'_\perp$ = –0.011 ± 0.003. Both values are found to be negative in the entire temperature range of the nematic phase.

## V. RESULTS OF THE ORDER PARAMETERS FOR THE TETRAPODE

The vibrational bands used are as follows: the carbonyl stretching vibrations at 1737 cm$^{-1}$, the phenyl stretching vibrations at 1608 cm$^{-1}$; and the out-of-plane deformations of the phenyl rings at 836 cm$^{-1}$ and 762 cm$^{-1}$. In principle the order parameters can be calculated by using only two bands. These are the in-plane vibrations 1608 cm$^{-1}$ and the out-of-plane deformations at 762 cm$^{-1}$. The transition dipole moment of the 1608 cm$^{-1}$ lies almost along the phenyl *para*-axis and for 762 cm$^{-1}$ band is directed normal to the long axis. However, the orientations of the transition moments within the molecular system essentially depend on the particular conformer under discussion. Hence the structure of the mesogenic group of the tetrapode was simulated in order to find possible conformers, and orientations of transition dipoles. This was done using Parallel Quantum Solution (PQS) package[16] (density functional theory (DFT) with Becke's hybrid three-parameter, Lee-Yang-Parr correlation functional -B3LYP). The standard Gaussian split-valence basis set with polarization and diffuse functions was used (6-31+G*). The energy difference found in between the different conformers is low, ∼0.5 kJ/mol, whereas the energy barrier separating the energy minima is ∼3 kJ/mol. This has been calculated from a scan of a dihedral (C-O-$C_{ar}$-$C_{ar}$) angle of the ester group. These calculations provide useful information about the orientation of the transition dipole moments within the mesogenic core. The x-ray study and molecular packing models[6] reveal that tetrapodes have the tendency to form platelets. In order to achieve an optimized packing of the constituents, the four ring mesogenic cores are tilted in the plane of the platelet (see Fig. 1(b)) that has $C_{2h}$ symmetry. Each platelet is formed such that the $a$ and $c$ dimensions of the platelet lie along the $x$ and $z$ directions, and these are of comparable lengths of the platelet in which the mesogens are tilted, and the $b$ dimension directed along the $y$-direction is of much smaller length. Locally, the mesogen cores are tilted within a well-defined plane and the phenyl rings are rather closer to this plane. It was found that 762 cm$^{-1}$ transition dipole moment makes on the average an angle of 18° with the y axis of the platelet. Figure 1(b) shows how the mesogenic units form a brick-like (platelet) structure. The mesogens are tilted in this structure such that the transition moment of the 1608 cm$^{-1}$ band makes an angle of $\beta$ with the platelet z axis and the transition dipole moment of the 762 cm$^{-1}$ band, transverse to the mesogen, makes an angle of 18° with the $y$ axis.

Figure 2(a) shows that the absorbance profiles of the bands 762 cm$^{-1}$ and 1737 cm$^{-1}$ are exactly orthogonal to that of 1608 cm$^{-1}$ band within the experimental error despite the fact that their corresponding transition dipoles are not perpendicular to the longitudinal transition dipole moment. The dependence of the IR absorbance on the polarization angle of the incident beam for several bands of the tetrapode system aligned planarly and homeotropically in the cell in a temperature range of 363 K–410 K is analyzed. All absorbance profiles show distinct absorbance anisotropy in the temperature range of the nematic phase where one of the minor directors in the absence of the external field coincides with the rubbing direction of the substrate. $A_Z$ is measured for the planarly aligned cell and the two components $A_X$, and $A_Y$ are measured for the homeotropic sample geometries. These are plotted in Fig. 2(b). The absorbance $A_0$ is measured in the isotropic phase for a particular band. In the nematic phase, we observe $A_X > A_Y$, for the 1608 cm$^{-1}$ band. This implies that the mesogenic cores have on the average, larger tilt fluctuations in the $X$-$Z$ plane compared to that in the $Y$-$Z$ plane. It is shown that $A_Z$ is greater than $A_X$, but both of these are greater than $A_Y$. In the $N$ phase of the tetrapode, where an interdigitation of the laterally attached mesogenic units is present, it is possible that the major director may be tilted. In order to determine whether or not it is tilted, the dependence of the absorbance for the phenyl ring deformations band at 762 cm$^{-1}$ vs. the angle of oblique incidence is investigated. The absorbance of this band plotted by open symbols in Fig. 2(a) shows that the angular profile is symmetrical with respect to the maximum that is observed at normal incidence (∼90°). This implies that the main director is directed along the $z$-axis. It seems that anisotropy in the tilt fluctuations originates from the shape of the platelet and not from the tilt of the director. If the dimensions $a$ and $c$ of the platelet are comparable to each other then the platelets align similarly to those of discotic molecules, i.e., edge-on lying along the rubbing direction.[17] It makes fluctuations in the disk-like plane easier than in the other two planes that are orthogonal to it. By comparing the absorbance components for the 1608 cm$^{-1}$ band in the planar and homeotropic cells, we find that the mesogenic cores in the homeotropic sample

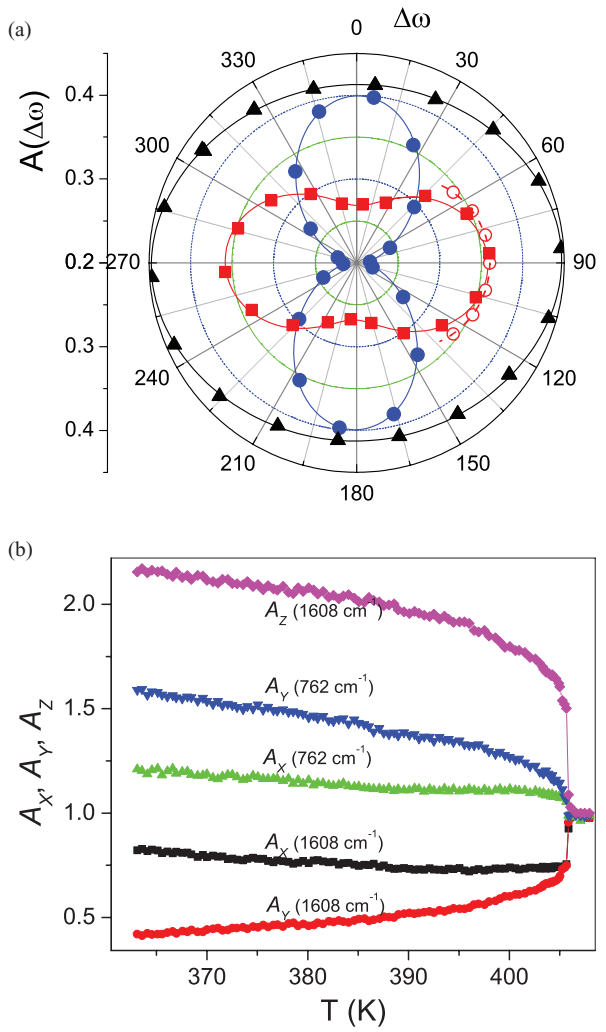


FIG. 2. (a) Polarisation angle $\Delta\omega$ dependence of the absorbance of the peak maximum A($\Delta\omega$):● for 1608 cm$^{-1}$ band, ■ for 762 cm$^{-1}$ and ▲ for 1737 cm$^{-1}$ band of the tetrapode at 373 K in the planar configuration of the cell. $\Delta\omega$ is measured with respect to the angle at maximum absorbance of the 1608 cm$^{-1}$ band. Absorbance vs. oblique incidence angle: ◯ for the 762 cm$^{-1}$ band (deformation of the phenyl ring) (b). Absorbance components normalized with those of the isotropic phase; $A_X$ (■), $A_Y$ (●), $A_Z$ (♦) values for phenyl ring stretching band 1608 cm$^{-1}$ and $A_X$ (▲), $A_Y$ (▼) for the phenyl out-of-plane band 762 cm$^{-1}$, measured for the homeotropically aligned sample.

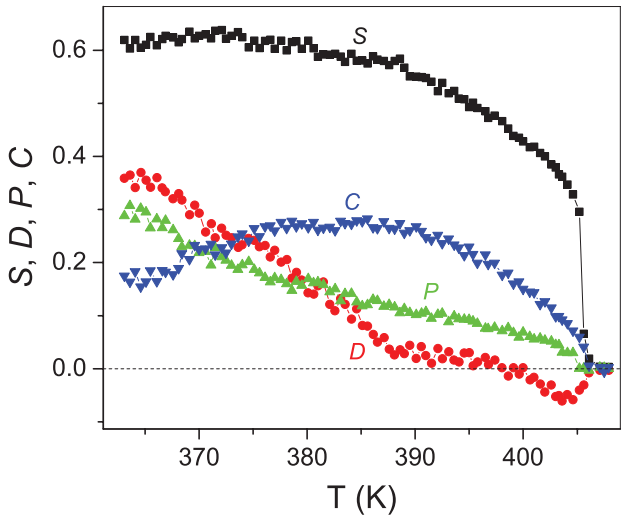


FIG. 3. Plot of order parameters of the tetrapode platelet; $S$ (■), $D$ (●), $P$ (▲) and $C$ (▼). All mesogens are assumed to be tilted in the $x$-$z$ plane of the platelet, $y$ axis of the platelet is chosen to be perpendicular to the tilt plane of the mesogens.

on the average are tilted by an angle $\beta$ with respect to the normal to the substrate (see Fig. 1(b)), and this angle increases from 30° to 39° as the temperature decreases. The results for the orientations of the transition dipole moments in the platelet are based on the IR results. The calculations for the order parameters $S$, $D$, $P$, and $C$ have been carried out using $A_X$, $A_Y$, and $A_0$ (for the two bands: 1608 cm$^{-1}$ and 762 cm$^{-1}$) given as inputs to Eq. (2).

The absorbance components of the terminal chains for symmetric and asymmetric $CH_2$ bands are used to calculate the order parameters $S$ and $D$ for the chains. These values confirm that the terminal chains are normal to the substrates in a homeotropic cell. The results of the absorbance components for terminal chains did not show any anisotropy in the $X$-$Y$ plane. Figure 3 shows the plot of the temperature dependence of the order parameters $S$, $P$, $C$, and $D$ determined for the tetrapode system. These indicate some interesting behavior of the system in the low temperature range: Both $S$ and $C$ parameters increase as we go down in temperature. In particular $C$ starts to decrease below $T$ = 380 K. The reason for this behavior is given as below. It seems that a gradual increase in the tilt of the mesogens makes the dimensions of the platelet ($c$ and $a$) along $z$ and $x$ directions comparable in length to each other (Fig. 1(b)). This obviously increases the fluctuation of the long axis in the $X$-$Z$ plane. This in turn increases the parameters $D$ and $P$ and decreases $S$ and $C$ as is found from their definitions.

The results for $S$ and $C$ given in Fig. 3 can also be explained by the molecular theory of the tetrapodes[5] These indicate that a relationship between the uniaxial and biaxial parts of the effective intermolecular interaction potential can be controlled by the tilt of the mesogenic groups. The phase diagram (Figs. 4 and 5 in Ref. 5) shows the dependence of the transition temperatures on the shape anisotropy or the tilt angle of the mesogens. Both phase diagrams contain a "triple" point where the three possible nematic phases (uniaxial calamitic nematic, uniaxial discotic nematic, and biaxial nematic) are in equilibrium with the isotropic phase. Significantly, the calamitic and discotic uniaxial nematic phases, presented in the phase diagrams, are composed of biaxial molecules of the same general structure but with different effective primary molecular axes. In the calamitic nematic phase, the primary molecular axis is parallel to the long axis of the platelet, while in the discotic nematic phase, the primary axis is chosen as the short axis of the platelet. This reorientation of the primary molecular axis is related to the fact that the molecule becomes more disk-like by increasing the tilt of the mesogenic groups (dimensions $a$ and $c$ of the platelet then become comparable to each other). The general tensorial character of the molecular theory enables one to easily convert the order parameters between the two molecular frames: between the calamitic and the discotic frames. It

can be shown that at low temperatures the $S_c$ (in the discotic frame) approaches a value of 0.6 while $S$ (in the calamitic frame) decreases below 0.6; thus the system close to the "triple" point really behaves as if it is in its discotic phase. Hence, we may say that when the order parameter $C$ saturates and then starts to decrease with temperature, the system be considered discotic rather than the calamitic one.

## VI. ELECTRIC FIELD INDUCED ROTATION OF THE MINOR DIRECTOR OF THE TETRAPODE IN ITS NEMATIC PHASE

The dependence of the rotation of the directors induced by the in-plane electric field is studied as a function of temperature and the amplitude of the electric field. A square wave signal of frequency 1 kHz and of voltage up to 700 V was applied across the gap between the two electrodes (i.e., in-plane field for the liquid crystal aligned in the homeotropic configuration). The in-plane switching of the tetrapode mesogen (in the same cell) observed under polarising optical microscope is shown in Fig. 4. In the absence of electric field, when the rubbing direction coincides with the polariser direction as in Fig. 4(a), the field of view is dark but it gradually gets brighter on increasing the electric field (Figs. 4(b)–4(d)). Then, we can rotate the LC cell to set the polariser parallel to the electric field (the rubbing direction is at the angle of ∼45° to the polariser). In the absence of electric field the field of view between the electrodes turns bright (Fig. 4(e)). On increasing the electric field, the field of view of the cell becomes gradually darker (Figures 4(f)–4(h)). On applying the electric field, the minor director initially oriented along the rubbing direction, is observed to rotate towards the direction of the applied electric field.

The rotations of both the major and minor directors are observed in IR spectroscopy through a gradual shift in the absorbance profiles vs. the angle of polarization for different vibrational bands. In particular, the absorbance profiles for the bands of 762 $cm^{-1}$, 836 $cm^{-1}$, 1737 $cm^{-1}$ enable us to obtain a direct insight into the dynamic behavior of the minor director. Strictly speaking, the position of the absorbance maximum at a particular temperature and electric field strength

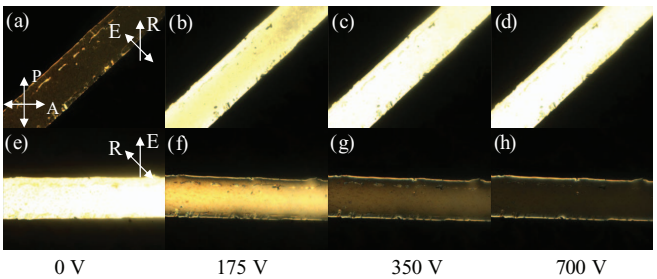


FIG. 4. Textures from a 5.2 $\mu$m thick rubbed homeotropic cell for a temperature of 363K. P = Polariser, A = Analyser and R = Rubbing, E = electric-field direction. The amplitudes of the signals are given below the images. (a), (b), (c), (d) are recorded for the cell rubbing direction parallel to the polariser, (e), (f), (g), (h) are recorded for the polariser parallel to the electric field direction. In the latter, the cell is rotated by an angle of 45°. The electrodes are made up of aluminium foils and are separated by a gap of 225 $\mu$m.

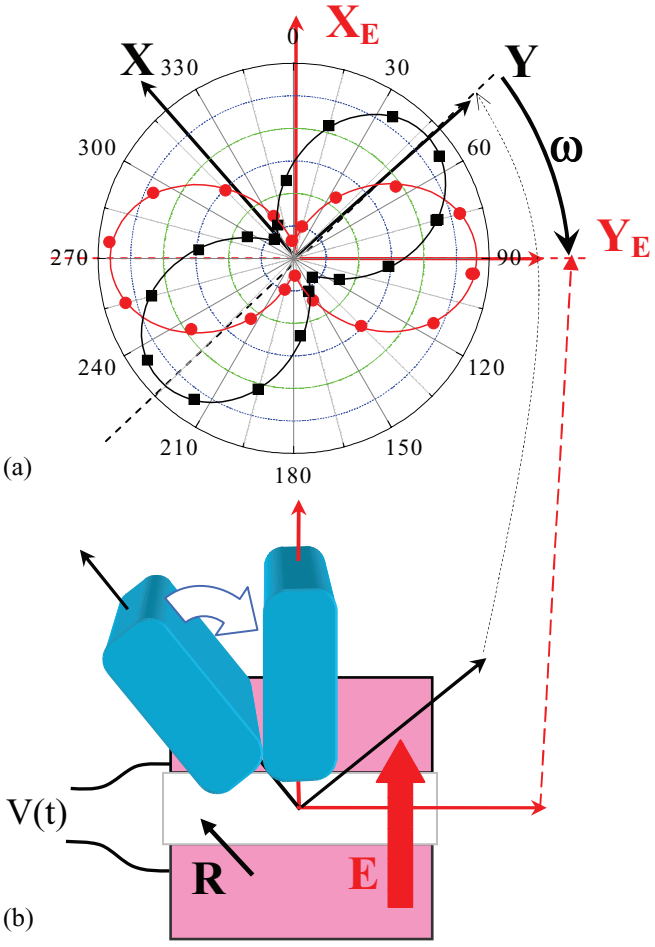


FIG. 5. (a) Polar plot of the 762 $cm^{-1}$ absorbance band before (●) and after (■) applying an electric field. (b) Configuration of the cell in the substrate plane ($X$–$Y$). E = electric field direction and R = rubbing direction. Blue boxes represent platelet orientations before and after applying an electric field. $X_E$ and $Y_E$ correspond to the axes of the profile with the electric field applied across X-axis.

indicates the favorable orientation of the corresponding transition dipole moment with reference to say the rubbing direction. For this the IR beam is incident in the $Z$ direction. The rotation of the minor director, coincident with the transverse dipoles, is observed through a gradual shift in the absorbance profile for the 762 $cm^{-1}$ vibrational band vs. the angle of polarization (Fig. 5(a)). Figure 5(b) shows the geometry of the cell in the ($X$-$Y$) plane of the substrate.

On increasing the field, we observed a gradual shift in the absorbance maximum for lateral dipole vectors (762 $cm^{-1}$ band and 1737 $cm^{-1}$) from the initial orientation normal to the rubbing direction to being normal to the electric field. Note that the secondary director along which the permanent dipole moment is directed, lies normal to the 762 $cm^{-1}$ vibration band. For large enough fields, this is directed along the electric field direction (see Fig. 5(a)). A similar behavior is observed for the 1608 $cm^{-1}$ band, except its maximum is shifted by 90° with respect to the corresponding absorbance maximum for the transverse dipole moment. Interestingly, the profiles of the 762 $cm^{-1}$ band rotate rather non-uniformly, particularly for $E = 0.7$ to 1.5 V/$\mu$m, (Fig. 6(a)).

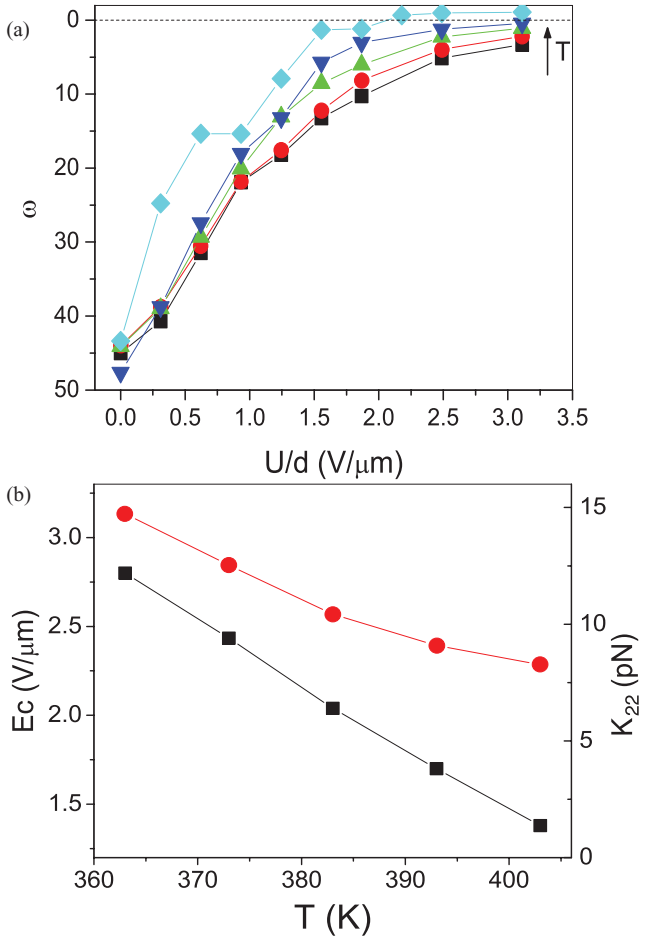


FIG. 6. (a) Electric field dependence of the rotation angle of the minor director for different temperatures: 363 K (■), 373 K (●), 383 K (▲), 393 K (▼) and 403 K (♦). The angle $\omega$ is defined as the orientation of the maximum of the 762 $cm^{-1}$ band with respect to the direction normal to the in-plane electrodes. In the Figure the arrow points to increasing temperature. (b) Temperature dependence of the critical electric field (■) necessary to switch the minor director by an angle $\cong 40^\circ$ and the elastic constant (●) for the reorientation of the secondary director towards the electric field.

In the nematic phase, the rotation of the minor director is due to the coupling of $E$ with $\Delta\varepsilon_\perp$ in the $XY$ plane. The rotation angle of the secondary director shows an almost thresholdless dependence on the amplitude of the electric field. This is due to a weak anchoring of the secondary director at the substrate ($W \cong 8$ $\mu$N/m). The evaluated threshold field varies from 0.22 V/$\mu$m to 0.17 V/$\mu$m in the temperature range of the nematic phase 363 K to 395 K. This indicates a rather weak temperature dependence of the elastic constants of the secondary director, though it is estimated with a rather limited accuracy. Therefore, it seems to be more accurate to measure the critical field necessary to rotate the secondary director to a particular orientation angle $\theta_m$ with respect to the direction of the field. The specific field can be evaluated using the integral over the $\theta$ angle of the director profile (in one elastic constant approximation).[18,19]

$$\int_{\theta_m}^{\theta_s} d\theta / \sqrt{\sin^2\theta_m - \sin^2\theta} = \frac{d}{\xi}$$

where $d$ is the cell thickness, $\theta_m$ and $\theta_s$ are the orientations of the director in the middle and at the substrate of the cell, respectively, $\xi = \sqrt{K_{22}/\varepsilon_0 E^2 \Delta\varepsilon_\perp}$ is the correlation length. The latter is described by the twist elastic constant $K_{22}$ of the secondary director, electric field $E$ and the static dielectric biaxiality $\Delta\varepsilon_\perp$. Both orientations of the director, $\theta_m$ and $\theta_s$, are measured under the polarizing microscope. For $\theta_m = 4^\circ$, $\theta_s$ is found to vary in between $8^\circ$ and $5.6^\circ$ in the temperature range 363 K–403 K (Fig. 6(b)). The angular limits are related to the anchoring energy by the formulae $\theta_s = \theta_m/(1-(\xi/L)^2)^{1/2}$, where $L = K_{22}/W$. $L$ is the elastic constant per unit of anchoring energy and can thus be calculated. The twist elastic constant $K_{22}$ together with its temperature dependence is of the same order of magnitude as of the elastic constants of a similar tetrapode system. The anchoring energy is found to decrease from 7.7 to 6.6 $\mu$N/m as the temperature increases.

## VII. DEPENDENCE OF THE ORDER PARAMETERS OF THE TETRAPODE ON THE ELECTRIC FIELD IN ITS NEMATIC PHASE

It is found that electric field affects the director orientation but the field also affects the orientational order parameters of the phase. All scalar order parameters show significant dependencies on the strength of the electric field (Figs. 7 and 8). The most clear observation is the increase in the nematic order parameter, $S$, which is related to that of the orientation of the long molecular axes with the field (Fig. 7(a)). The carbonyl dipole moments have major influence on the sign of the dielectric anisotropy. The large dipole moments of the lateral carbonyl groups enable the system to exhibit significant negative dielectric anisotropy. An application of the in-plane electric field decreases the tilt angle of the mesogenic core and stabilizes the homeotropic alignment. Large field induced increase of the nematic order parameter can be explained by the cooperative interactions of dipoles (lying within a correlation length).[6] The change in $S$ should be matched by a significant change at the $I$-$N$ transition too. However, we could not approach the $N$-$I$ transition on increasing the temperature as a strong hydrodynamic flow was induced by the electric field close to the $N$-$I$ transition temperature. The molecular biaxiality parameter, $D$, exhibits an interesting dependence on the electric field (Fig. 7(b)). Significantly, large positive values of the molecular biaxiality, $D$, are observed at lower temperatures and this tendency disappears at higher temperatures. For the latter, $D$ initially goes slightly negative (for reasonable low fields) and then becomes significantly negative, $D \sim -0.3$, for larger fields. It seems that the electric field quenches fluctuation of the $x$-axis (which lies along the electric dipole moment direction) thus decreasing $S^Z_{xx}$ while $S^Z_{yy}$ remains unchanged.

The *extrinsic* biaxiality parameter, $P$, remains almost unaltered at higher temperatures with a small decrease observed for moderate fields (Fig. 8(a)). At lower temperatures, however, $P$ decreases significantly and then increases well above its initial level. Such an observed behavior may indicate that the magnitude of the applied field is not large enough to complete the reorientation of the minor director. For a moderate

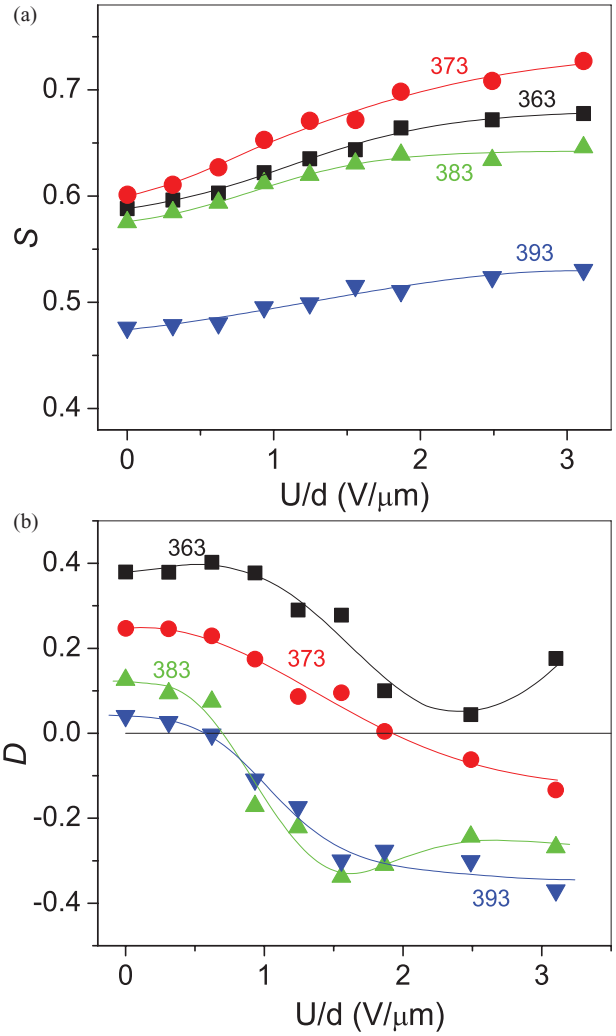


FIG. 7. Order parameters: $S$, and $D$ vs. electric field for different temperatures for a weakly rubbed cell (rubbing strength 60 mm): 363 K (■), 373 K (●), 383 K (▲) and 393 K (▼).

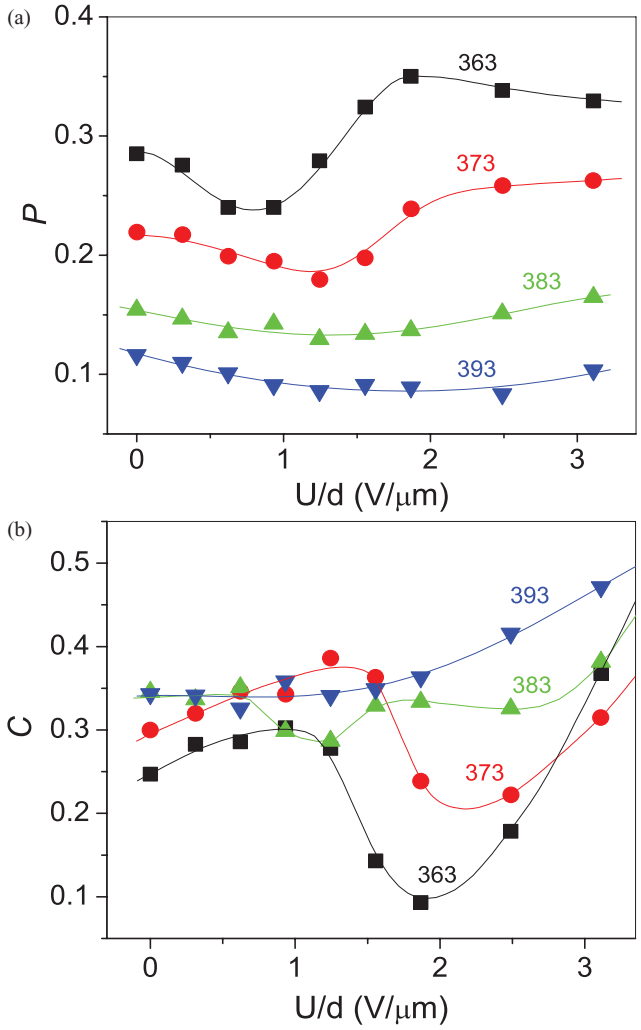


FIG. 8. Order parameters: $P$ and $C$ vs. electric field for different temperatures for a weakly rubbed cell (rubbing strength 60mm): 363 K (■), 373 K (●), 383 K (▲) and 393 K (▼).

electric field; an equilibrium state is not reached. The *intrinsic* biaxiality parameter, $C$, at the low temperatures decreases by a factor of two and then grows to a higher value compared to even its initial value (Fig. 8(b)). On going to higher temperatures and higher fields, this trend continues. This behavior may correspond to the field at which the molecular biaxiality, $D$, becomes negative. It seems that the minor director does not rotate uniformly with an increase in the electric field. Initially, the electric field destroys an existing order and then builds up the order of the minor axes in the direction of the field. It has to be noted that a moderate field is not large enough to complete the rotation during the half period of the field. But when the field is large enough (>2.5 V/$\mu$m), the maxima of the angular profile for the 762 cm$^{-1}$ band rotates by an angle of ~45° and the electric field then takes an entire control over the alignment of the major and minor directors. However, one needs to apply much higher fields in order to obtain saturation in the phase biaxiality. Since the tetrapode has a negative dielectric anisotropy, one should expect a significant growth in the nematic and the biaxial order parameters with an increase of the in-plane electric field.

## VIII. SUMMARY

The dependence of the IR absorbance on the polarization angle for several IR bands is investigated. The IR absorbance profiles plotted as a function of polarization angle show distinct anisotropy in the range of the nematic phase. Results show that the tetrapodes have tendency to pack their mesogenic cores in a plane in such a way that the mesogens form platelets. This is supported by x-ray investigations and by the molecular packing models. The mesogenic cores are tilted by an angle varying from 30° to 39°, with respect to the normal to the substrate. The tilt angle increases as the temperature decreases. For zero field the temperature dependencies of the order parameters $S$ and $C$, for the nematic and biaxial order show rather unexpected results. These parameters saturate at a temperature of about 380 K and then start to decrease. Such a behavior is consistent with the molecular theory of the organo-siloxane tetrapodes.[5] As temperature decreases, the tilt of the mesogenic core increases, the tetrapode molecules become more disk-like and the system has to be described by the right side of the phase diagram (see Fig. 4 of Ref. 5) and the phase thus formed corresponds to a discotic nematic phase.

For the liquid crystal in homeotropic configuration and when an in-plane electric field of frequency 1 kHz is applied across the gap of the electrodes, the rotation of the minor director is observed through the angular shifts of the absorbance profiles of the lateral transition dipole moments. We observe a gradual shift in the absorbance *minimum* from the orientation of the minor director along the rubbing direction towards the direction of the electric field. Note that the lateral transition dipole moment is normal to the secondary (minor) director. The minor director does not rotate uniformly with an increase in the electric field. Initially, the electric field destroys an existing order and then builds up the order of the minor axes in the direction of the field. A moderate field in not large enough to complete the rotation within a half period of the field. Only the field above the threshold enables the rotation of the minor director to occur by an angle of $\sim 45^{\circ}$. All scalar order parameters show significant dependencies on the strength of the electric field. Both increase in the order parameter $S$ and a decrease in $P$ clearly originate from the negative dielectric anisotropy of the material. An application of an in-plane electric field reduces the tilt of the mesogens and thus stabilizes the homeotropic alignment of the sample. The molecular biaxiality, $D$, is positive at low temperatures and low fields, this goes to zero and then to negative values. $D$ tends to vanish at higher temperatures on increasing the electric field. The biaxiality parameter, $C$, at the low temperatures decreases by a factor of two and then grows higher than its initial value. On going to higher temperatures and higher fields, this trend continues. This result may correspond to the field at which the molecular biaxiality, $D$, becomes negative. It seems that changes in the $D$, $P$, and $C$ parameters are mostly due to a quenching of the effective electric dipole moment which is being directed along the field directions as the field increases. However, one needs to apply much larger fields to saturate the phase biaxiality. Since the tetrapode itself has negative dielectric anisotropy, a significant growth in the nematic and the biaxial order parameters as expected is observed with an increase the magnitude of the in-plane electric field.

## ACKNOWLEDGMENTS

Collaboration between Dublin and Hull was funded by the BIND EU project FP7 No. 216025. The authors thank G. R. Luckhurst, and M. A. Osipov for discussions. K. Merkel and A. Kocot thank the Polish Scientific Research Committee (KBN) for the award of grant N202 282734. The Science Foundation of Ireland is thanked for the award of Walton Professorship to A. Kocot (07/W.1/I1833).

[1] K. Merkel, A. Kocot, J. K. Vij, R. Korlacki, G. H. Mehl, and T. Meyer, Phys. Rev. Lett. **93**, 237801 (2004).
[2] J. L. Figueirinhas, C. Cruz, D. Filip, G. Feio, A. C. Ribeiro, Y. Frère, T. Meyer, and G. H. Mehl, Phys. Rev. Lett. **94**, 107802 (2005).
[3] D. Filip, C. Cruz, P. J. Sebastiao, A. C. Ribeiro, M. Vilfan, T. Meyer, P. H. J. Kouwer, and G. H. Mehl, Phys. Rev. E **75**, 011704 (2007).
[4] K. Neupane, S. W. Kang, S. Sharma, D. Carney, T. Meyer, G. H. Mehl, D. W. Allender, S. Kumar, and S. Sprunt, Phys. Rev. Lett. **97**, 207802 (2006).
[5] M. V. Gorkunov, M. A. Osipov, A. Kocot, and J. K. Vij, Phys. Rev. E **81**, 061702 (2010).
[6] D. Filip, C. Cruz, P. J. Sebastiao, M. Cardoso, A. C. Ribeiro, M. Vilfan, T. Meyer, P. H. J. Kouwer, and G. H. Mehl, Phys. Rev. E **81**, 011702 (2010).
[7] D. A. Dunmur and H. Toriyama in *Handbook of Liquid Crystals*, edited by D. Demus, J. Goodby, G. W. Gray, H.-W. Spiess, and V. Vill, (Wiley-VCH, Weinheim, 1998) Vol. 1, Chap. VII.1, p. 189.
[8] J. W. Emsley *Nuclear Magnetic Resonance of Liquid Crystals* (D. Reidel, Dordrecht, 1983), p. 379.
[9] C. Zannoni in *The Molecular Dynamics of Liquid Crystals*, edited by G. R. Luckhurst and C. A. Veracini, (Kluwer, Dordrecht, 1994), p. 34.
[10] B. K. P. Scaife and J. K. Vij, J. Chem. Phys. **122**, 174901 (2005); A. Kocot, R. Wrzalik, and J. K. Vij, Liq. Cryst. **21**, 147 (1996).
[11] J. P. Straley, Phys. Rev. A **10**, 1881 (1974).
[12] P. K. Karahaliou, A. G. Vanakaras, and D. J. Photinos, J. Chem. Phys. **131**, 124516 (2009).
[13] K. Miyachi, J. Matsushima, Y. Takanishi, K. Ishikawa, H. Takezoe, and A. Fukuda, Phys. Rev. E **52**, R2153 (1995); A. Kocot, R. Wrzalik, B. Orgasinska, T. Perova, J. K. Vij, and H. T. Nguyen, Phys. Rev. E **59**, 551 (1999).
[14] K. Merkel, A. Kocot, J. K. Vij, G. H. Mehl, and T. Meyer, J. Chem. Phys. **121**, 5013 (2004).
[15] A. Kocot and J. K. Vij, Liq. Cryst. **37**, 653 (2010); E. Hild, A. Kocot, J. K. Vij, and R. Zentel, Liq. Cryst. **16**, 783 (1994); M. D. Ossowska-Chruściel, R. Korlacki, A. Kocot, R. Wrzalik, J. Chruściel, and S. Zalewski, Phys. Rev. E **70**, 041705 (2004).
[16] P. Pulay, J. Baker, and K. Wolinski, Parallel Quantum Solutions; see http://www.pqs-chem.com.
[17] T. S. Perova, J. K. Vij, and A. Kocot, Europhys. Lett. **44**, 198 (1998); T. S. Perova and J. K. Vij, Adv. Mater. **7**, 919 (1995).
[18] G. Barbero and L. R. Evangelista, *An Elementary Course on the Continuum Theory for Nematic Liquid Crystals* (World Scientific, Singapore, 2001).
[19] R. Stannarius, A Eremin, M. G. Tamba, G. Pelzl, W. Weissflog, Electronic-Liquid Crystal Communications, see www.e-lc.org/docs/2006_06_05_36_17.